# Effects of Cyclic-Hydrocarbon Substituents and Linker Length on Physicochemical Properties and Reorientational Dynamics of Imidazolium-Based Ionic Liquids

Toshihiko Mandai,[†] Akiko Matsumura,[†] Mamoru Imanari,[‡] and Keiko Nishikawa*,[†]

[†]Department of Nanomaterial Science, Graduate School of Advanced Integration Science and [‡]Chemical Analysis Center, Chiba University, 1-33 Yayoi, Inage-ku, Chiba 263-8522, Japan

Ⓢ Supporting Information

ABSTRACT: We synthesized a series of alkylimidazolium-based ionic liquids (ILs) incorporating cyclopentyl, cyclohexyl, or phenyl groups as nonionic units substituted on an acyclic alkyl linker and characterized them with respect to physicochemical properties and reorientational dynamics. The effects of the nonionic substituents and linker length on the properties of these ILs were carefully examined. The physicochemical properties of the ILs are found to partially reflect the properties of the nonionic substituents. While the liquid densities showed a similar trend in linker-length dependence of each series of ILs, a distinct trend was observed for the shear viscosities of them. By comparison of correlation times obtained by ^{13}C NMR spectroscopy, it is revealed that elongation of the linkers influences the characteristic effects of the nonionic substituents on the reorientational dynamics of the system.
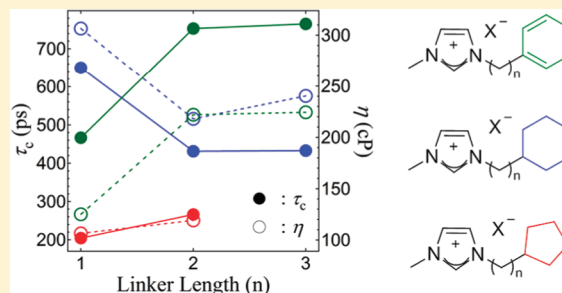
1. INTRODUCTION

Ionic liquids (ILs) have been receiving considerable attentions owing to their diverse potential to serve as alternatives for conventional materials.[1−7] Although many applications of ILs have been developed, fundamental studies leading to an understanding of these substances have not been sufficient. Because most ILs are composed of organic ions, their functionalities and physicochemical properties can be tuned by simple chemical modification.[2,8−13] Thus, it is crucial to clarify the correlation between the chemical structures and physicochemical properties of ILs.

An *n*-alkyl linker is a fragment that links two or more functional units, and consequently, it may have unique physicochemical features distinct from typical *n*-alkyl groups. Because linear linkers can control the configuration and distance between the substituents, they have been intensively investigated in various chemical fields, such as liquid crystals, pharmaceuticals, and polymers.[14−21] For example, typical mesogenic dimer molecules are composed of rigid aromatic groups and flexible chains, and their phase transitional properties are known to depend on the length of the flexible chain and show a characteristic even−odd effect.[14−18] Contrary to the large volume of linker studies in other molecular systems, only a few reports providing information on linkers in ILs are available, such as those investigating dicationic and zwitterionic ILs.[22−25] Previously, it was reported that bis-imidazolium ILs showed a unique *n*-alkylene linker-length dependence of the thermal properties and shear viscosities.[24] In those series, because both ends of the linkers were substituted by ionic imidazolium cations, interionic interactions between the two

cations influenced the natures of the linkers. Thus, it is important to examine linkers in various systems to develop a comprehensive understanding of the linker effects on ILs.

In this study, we focused on systems having linkers with both ionic and nonionic cyclic substituents. To investigate the linker effects on these systems, a variety of alkylimidazolium-based ILs with cyclic hydrocarbons at one end of an alkyl chain and an imidazolium substituent at the other were synthesized and characterized with respect to physicochemical properties and reorientational dynamics. To elucidate the effects of the chemical environment around the linkers on the physicochemical features of the linkers, the dependence of the linker length as well as the nonionic substituents on these features was carefully examined. Three functional groups were chosen as the nonionic substituents: cyclopentyl, cyclohexyl, and phenyl groups. Hereafter, the series of imidazolium ILs are abbreviated as **Cyp[*n*]X**, **Cyh[*n*]X**, and **Ph[*n*]X**, in which **Cyp[*n*]**, **Cyh[*n*]**, and **Ph[*n*]** denote imidazolium cations having cyclopentyl, cyclohexyl, and phenyl groups as the nonionic substituents, respectively, where *n* denotes the length of the *n*-alkyl linker. These imidazolium cations were paired with the bis-(trifluoromethanesulfonyl)amide (NTf_2) anions to obtain liquid salts at ambient temperature.

We evaluated the overall molecular dynamics because the reorientational component can dictate the physicochemical properties of ILs in the liquid state. In general, because the

relaxation times provide valuable information on relatively slow dynamics, NMR spectroscopy is one of the most powerful methods to study the reorientational dynamics of ILs.[26−30] NMR spectroscopy was performed with various imidazolium ILs. By comparing the longitudinal relaxation times of ^{13}C nuclei (^{13}C-T_1) and the correlation times (τ_c) of the carbons constituting the linkers and nonionic substituents of the series of imidazolium ILs, we evaluated the reorientational dynamics of these segmental carbons.

2. EXPERIMENTAL SECTION

2.1. Synthesis and Characterization. Figure 1 displays the chemical structures of the series of imidazolium-based ILs
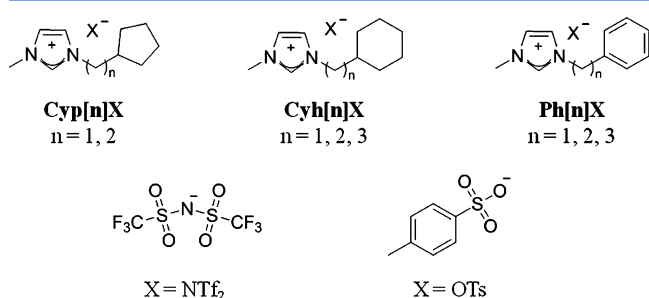
Figure 1. Chemical structures of **Cyp[*n*]X**, **Cyh[*n*]X**, and **Ph[*n*]X**.

synthesized in this study. The abbreviations for each imidazolium IL are also listed. As shown in the figure, a typical NTf₂ anion was chosen for this study, resulting in liquid salts at ambient temperature. The ILs with tosylate (OTs) anions, as the precursors of the ILs with NTf₂ anions, were synthesized by reacting methylimidazole with the respective *p*-toluenesulfonate derivatives having the desired nonionic substituents.

Complete synthetic procedures for each imidazolium IL and their analytical data are provided in the Supporting Information. All of the imidazolium ILs were synthesized according to previously published reports.[31,32] Their molecular structures and purities were assigned by NMR spectroscopy and elemental analyses. NMR spectra were recorded in dimethylsulfoxide-d_6 (DMSO-d_6) or chloroform-*d* on a JEOL JNM-LA 500 spectrometer and a JEOL JNM-LA 400 spectrometer with a ^{1}H resonance frequency of 500 and 400 MHz, respectively. The chemical shifts of ^{1}H and ^{13}C signals were obtained relative to TMS as the internal standard. The ^{1}H and ^{13}C signals of **Cyp[*n*]NTf₂**, **Cyh[*n*]NTf₂**, and **Ph[*n*]NTf₂** were assigned on the basis of [1]H−^{1}H COSY and [1]H−[13]C HMQC spectra. The spectra for all products showed high sample purity, and no extra peaks were observed. Elemental analyses were performed on a Perkin-Elmer 2400 and CE 440F apparatus. All deviations from the calculated values were less than ±0.3%.

2.2. Measurements. The water contents of the ILs were estimated by Karl Fischer titration using a Mettler Toledo Karl Fischer Coulometer. The water contents of all ILs were less than 150 ppm. Thermal properties, such as glass transition temperatures (T_g) and melting points (T_m), were determined by differential scanning calorimetry (Rigaku, Thermo plus Evo). A scanning rate of 10 K/min and a measured temperature range of 173−423 K were employed. The onset of the change in heat capacity was considered as T_g. The T_m values were obtained at the top of the corresponding endothermic peaks. An oscillating U-tube densitometer (Anton Paar, DMA 4500)

was used for liquid density measurements. Shear viscosity measurements were performed using a falling-ball viscometer (Anton Paar, AMVn). Both liquid densities and shear viscosities of the imidazolium ILs were measured at 298 K.

To evaluate the reorientational dynamics of the different imidazolium ILs, ^{13}C-T_1 was measured on a JEOL LA-400 spectrometer with the ^{13}C resonance frequency of 100 MHz. To measure ^{13}C-T_1, samples were prepared by placing each IL in a sample tube with an outer diameter of 4 mm, drying the sample under a vacuum of 1 Torr at 313 K for 24 h, and then flame sealing the tube. The 4 mm sample tube was inserted into a 5 mm standard NMR sample tube. DMSO-d_6 for a field/frequency lock was infused in the narrow space between the 4 and 5 mm tubes. The ^{13}C-T_1 values of each carbon in the linkers and the nonionic substituents were obtained as a function of temperature in the range of 303−393 K under the ^{1}H broad-band decoupling condition by the inversion recovery method.[27] The measurements were performed three times, and all deviations in the experimental values from the average were within ±3%. The τ_c values of each carbon were obtained from the temperature-dependent ^{13}C-T_1 results.

Crystals of **Cyp[1]OTs**, **Cyh[1]OTs**, and **Cyh[2]OTs** that were suitable for single-crystal X-ray analysis were obtained from an ethanol/diethyl ether solution or acetonitrile/diethyl ether solution. Although conformational structures of cations would change by exchange of paired anion species, determination of the structures of these imidazolium ILs in the crystalline state enables the clarification of some important structural aspects of the linkers and substituents. Thus, we performed single-crystal X-ray analyses. X-ray diffraction data were collected on a Bruker APEX II CCD area detector using Mo Kα (λ = 0.71073 Å) radiation. Because of the high hygroscopicity of the crystals, each single crystal was mounted on a glass pin coated with a minimal amount of manicure to avoid adsorbing moisture and cooled to 173 K by a stream of nitrogen gas. The crystal structures were determined by direct method SHELXS-97 and refined by full-matrix least-squares SHELXL-97.[33] Non-hydrogen atoms were refined anisotropically, and hydrogen atoms were included in their calculated positions.

3. RESULTS AND DISCUSSION

3.1. Physicochemical Properties. Table 1 summarizes the physicochemical properties determined in this study for the series of alkylimidazolium ILs with nonionic substituents linked to the imidazolium cation via an alkylene linker.

3.1.1. Density. It is clear from Table 1 that the order of the liquid densities is as follows: **Ph[*n*]NTf₂** > **Cyp[*n*]NTf₂** > **Cyh[*n*]NTf₂**. For the corresponding hydrocarbons, the order of the densities differs from that of the ILs (benzene (Ph) > cyclohexane > cyclopentane).[34] This trend is explained in terms of the van der Waals volume (V_{vdw}), excluded volume (V_{ex}), and interactions. V_{vdw} values are calculated using the van der Waals increment, van der Waals radii, and bond lengths.[35−37] The calculated V_{vdw} values of cyclopentane, cyclohexane, and benzene are 85.0, 102.0, and 80.3 Å³, respectively. In addition, the molecular shape of benzene is completely planar, whereas those of cycloalkanes are nearly spherical, resulting in a smaller V_{ex} for benzene than that for the two cycloalkanes. Because smaller V_{vdw} and V_{ex} values lead to a higher filling fraction in the liquid, the density of benzene is higher than those of the two cycloalkanes. The higher density values of **Ph[*n*]NTf₂** in comparison with those of the analogous cycloalkyl ILs can be

**Table 1. Physicochemical Properties of Cyp[n]NTf₂, Cyh[n]NTf₂, and Ph[n]NTf₂**

ILs	MW (g/mol)	$T_g{}^a$ (K)	$T_m{}^a$ (K)	density^b (g/cm³)	shear viscosity^b (cP)
Cyp[1]NTf₂	445.4	200.2	n. o.	1.438	106.4
Cyp[2]NTf₂	459.4	198.9	n. o.	1.408	119.1
Cyh[1]NTf₂	459.4	212.1	n. o.	1.414	306.6
Cyh[2]NTf₂	473.5	207.1	n. o.	1.386	218.0
Cyh[3]NTf₂	487.5	207.5	n. o.	1.358	240.4
Ph[1]NTf₂	453.4	215.8	n. o.	1.489	125.0
Ph[2]NTf₂	467.4	214.4	n. o.	1.456	222.0
Ph[3]NTf₂	481.4	212.7	n. o.	1.434	224.4

$^a T_g$ and T_m represent the glass transition temperature and melting point, respectively. ^{b}Densities and shear viscosities were measured at 298 K.

explained in terms of these V_{vdw} and V_{ex} effects. On the other hand, as previously reported,[38] the densities of the Cyp[n]NTf₂ ILs are higher than those of the Cyh[n]NTf₂ ILs because of a higher charge density of the cations with cyclopentyl groups. For typical hydrocarbons, their liquid densities increase as their carbon number increases. The reason for this phenomenon is attributed to the fact that van der Waals interactions among hydrocarbon molecules are enhanced as the carbon number increases. Thus, it is suggested that the density dependence on the carbon number for Cyp[n]NTf₂ and Cyh[n]NTf₂, which is distinct from what is observed for the respective hydrocarbon molecules, is attributed to a difference in the interactions that dominantly influences the densities.

A similar linker-length dependence of the densities was observed in the series of alkylimidazolium ILs irrespective of the nonionic substituents. As reported in Table 1, the densities of the ILs decrease as the length of the linkers increases. It is well-known that liquid densities of typical 1,3-dialkylimidazolium ILs decrease as the alkyl length increases.[8,9] Moreover, the densities of bis-imidazolium-based dicationic ILs also decrease with the elongation of the alkylene linker.[22,24] These results indicate that the linkers and n-alkyl chains have similar effects on the liquid densities of ILs in terms of the carbon number.

3.1.2. Shear Viscosity. The linker-length dependence on the shear viscosities for a series of imidazolium ILs is shown in Table 1 and Figure 2. In the series with the linker length of n =
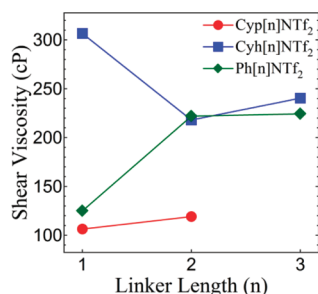
Figure 2. Linker-length dependencies of shear viscosities for Cyp[n]NTf₂, Cyh[n]NTf₂, and Ph[n]NTf₂ at 298 K.

1, the order of the shear viscosities for the ILs is as follows: Cyh[1]NTf₂ > Ph[1]NTf₂ > Cyp[1]NTf₂. In this case, the order of the shear viscosities of the ILs is consistent with that of the respective hydrocarbons.[34] This fact indicates that the shear viscosities for these imidazolium ILs reflect the properties of the nonionic substituents themselves. Moreover, it has been reported that the flexibility of the substituents strongly affects the viscosities of ILs.[8,39] Thus, it is suggested that the effect of insertion of a methylene linker on the flexibility of the nonionic substituents is small.

Contrary to what was observed for the liquid densities, a distinct trend in linker-length dependence was observed for the shear viscosities of each series of imidazolium ILs. The linker-length dependence of the shear viscosities for Cyh[n]NTf₂ is similar to the case of 1,3-dialkylimidazolium ILs,[8,9,12] while the results for Cyp[n]NTf₂ and Ph[n]NTf₂ are different, showing a simple increase in the shear viscosities as the linker length increases. From a structural perspective, the mobilities of the linkers in Cyp[n]NTf₂, Cyh[n]NTf₂, and Ph[n]NTf₂ are expected to be comparable when they have the same number of carbons. This suggests that the distinct linker-length dependence is not attributed to the mobility of the linkers themselves but to the effect of the linker length on the mobility of the nonionic substituents and the entire cation. The reorientational dynamics, which strongly correlate to the mobility and viscosity of substances, can be evaluated by NMR spectroscopy. The dynamics of the linkers and the nonionic substituents are discussed in section 3.2.

3.1.3. Thermal Properties. All of the imidazolium ILs showed only a glass transition without crystallization under the scanning conditions used herein. The T_g values of the Cyp[n]NTf₂ series are lower than those of the other series, and this result is expected owing to the lower shear viscosities of the series.

The thermal properties and crystal structures of the imidazolium ILs paired with OTs anions, which were the precursors for the ILs with NTf₂ anions, were also studied because they may provide some useful information. The thermal and crystallographic data of them are summarized in the Supporting Information. On the contrary to the ILs with NTf₂ anions, the OTs ILs were obtained as solids in which the Cyp[n]OTs and Cyh[n]OTs ILs were crystalline solids and the Ph[n]OTs ILs were waxy ones. For the crystalline ILs of n = 1, the T_m value of Cyh[1]OTs is higher than that of Cyp[1]OTs as well as the ILs incorporating cycloalkyl groups without linkers at the N-position of the imidazolium cations.[38] Moreover, there was a difference between the Cyp[n]OTs and Cyh[n]OTs ILs with respect to the linker-length dependence of T_m. The cause of these phenomena can be explained in terms of the crystal structures and mobility of the cations.

3.2. Reorientational Dynamics. Reorientational dynamics is known to strongly influence the viscosities of viscous liquids. Thus, to evaluate the reorientational dynamics, the temperature dependence of ¹³C-T_1 for the series of NTf₂ ILs was measured by NMR spectroscopy. In general, ¹³C-T_1 has several relaxation mechanisms, and thus, the T_1 value is composed of multiple components. The T_1 value is described as follows

$$\frac{1}{T_1} = \frac{1}{T_1^{DD}} + \frac{1}{T_1^{CSA}} + \frac{1}{T_1^{SR}} + \frac{1}{T_1^{SC}} + \frac{1}{T_1^{Q}} \qquad (1)$$
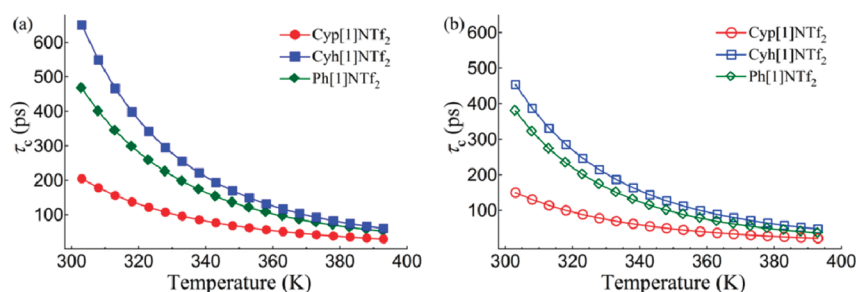
Figure 3. Temperature dependencies of (a) τ_c of the linker carbons and (b) average τ_c values of the carbons constituting each nonionic substituent for **Cyp[1]NTf$_2$, Cyh[1]NTf$_2$,** and **Ph[1]NTf$_2$.**

where T_1^{DD} is the dipolar−dipolar relaxation, T_1^{CSA} is the chemical shift anisotropy, T_1^{SR} is the spin rotation relaxation, T_1^{SC} is the scalar relaxation, and T_1^Q is the electric quadrupole interaction. Because the T_1^Q mechanism is significant only when the nuclei contain spins over 1/2, the contribution from T_1^Q can be neglected. T_1^{SC} has effects on T_1 relaxation when the chemical exchange occurs. Although the cyclohexyl group possesses the conformational interconversion, the most stable conformation practically occupies the populations because of the high activation energy of the interconversion.[40,41] Thus, the term of T_1^{SC} is negligible. The T_1^{SR} mechanism becomes important only for the relaxation of gas molecules. When the samples have double bonds, aromatic groups, or carbonyl carbons, the contribution from T_1^{CSA} to the T_1 value may be necessary to examine. Our samples in this study contain cations involving aromatic imidazolium moieties. Then, we evaluated the term of T_1^{CSA} by comparing the T_1 values obtained by using a spectrometer with the ^{13}C resonance frequency of 150 MHz with those of 100 MHz. As a result, the contribution of T_1^{CSA} to the ^{13}C-T_1 values was within the experimental error, which was several percent. In addition, the cross-relaxation effect on the dipolar−dipolar relaxation mechanism of ^{13}C-T_1 under the proton-decoupling condition is also considerably small.[42] Therefore, we assume that the observed ^{13}C-T_1 values depend primarily on T_1^{DD}. Then, ^{13}C-T_1 values can be described by the following equation for the dipolar−dipolar relaxation mechanism[28,43]

$$\frac{1}{T_1} = \frac{1}{T_1^{DD}}$$

$$= \frac{1}{20} N_H \left(\frac{\mu_0}{4\pi}\right)^2 \frac{\gamma_C^2 \gamma_H^2 \hbar^2}{r^6} \times \left[\frac{2\tau_c}{1 + (\omega_C - \omega_H)^2 \tau_c^2} \right.$$

$$\left. + \frac{2\tau_c}{1 + \omega_C^2 \tau_c^2} + \frac{12\tau_c}{1 + (\omega_C + \omega_H)^2 \tau_c^2} \right] \quad (2)$$

where μ_0 is the permittivity of vacuum; γ_C and γ_H are the gyromagnetic ratios of the ^{13}C and ^{1}H nuclei, respectively; $\hbar$ is $h/2\pi$, where h is Planck's constant; r is the distance between a carbon and a directly bonded proton; τ_c is the rotational correlation time; and ω_C and ω_H are the resonance frequencies of the ^{13}C and ^{1}H nuclei, respectively. It can be considered that the temperature-dependent ^{13}C-T_1 values are a function of the correlation time. The correlation times obey the Arrhenius equation[27,30]

$$\tau_c = \tau_0 \exp\left(\frac{E_a}{RT}\right) \quad (3)$$

where τ_0 is the correlation time at an extremely high temperature, E_a is the activation energy, and R is the gas constant. In general, the dipolar−dipolar relaxation mechanism for viscous liquids is dominated by molecular reorientation involving anisotropic molecular motion and intramolecular segmental motion.[44] Thus, τ_c represents the reorientational dynamics.

The temperature dependence of the τ_c values of the linkers and the nonionic substituents for **Cyp[1]NTf$_2$, Cyh[1]NTf$_2$,** and **Ph[1]NTf$_2$** is displayed in Figure 3a and b. For the nonionic substituents, these values are represented as averages of the τ_c values of all carbons constituting each nonionic substituent except for **Ph[1]NTf$_2$**. In the case of **Ph[1]NTf$_2$**, because the carbon bonded to the linker has no directly bonded proton, the dipole interaction is too small to contribute to the relaxation mechanism of this carbon. In fact, the measured ^{13}C-T_1 of this carbon is considerably long, and as a result, it significantly affects the average ^{13}C-T_1 value of the phenyl group (Figures S4 and S5, Supporting Information). For this reason, the τ_c value of the phenyl group is considered as the average of the τ_c values of the carbons having directly bonded protons.

It is clear from Figure 3 that the order of the τ_c values of the ILs at the same temperature is as follows: **Cyp[1]NTf$_2$** < **Ph[1]NTf$_2$** < **Cyh[1]NTf$_2$**. This order is consistent with that of their shear viscosities. As described above, the term of T_1^{CSA} in the imidazolium and phenyl carbons is sufficiently small to be negligible in the ^{13}C-T_1 values. Thus, the τ_c values of each nonionic substituent are representative of the segmental motion component of the molecular reorientation. On the other hand, the segmental motion of the linkers might be restricted by the substituents on both of their ends. In fact, the mobility of the methylene group inserted between the imidazolium cation and the cyclohexyl group is considerably low, leading to a high shear viscosity in the corresponding IL.[31] Thus, it can be concluded that the mobility of the entire cations including the nonionic substituents, rather than the segmental motion of the linkers, dominates the shear viscosities for the series of ILs with the linker length of $n = 1$.

Next, we examined the linker-length dependences of τ_c, and the results for **Cyp[n]NTf$_2$, Cyh[n]NTf$_2$,** and **Ph[n]NTf$_2$** at 303 K are displayed in Figure 4. The τ_c values of the linkers are considered as the average of all τ_c values of each linker component, and those of the nonionic substituents are determined in the same manner as shown in Figure 3. Initially, we focus on the results of **Cyp[n]NTf$_2$** (Figure 4a) and **Ph[n]NTf$_2$** (Figure 4c). They showed a similar linker-length dependence of the τ_c values of both the linkers and nonionic substituents, with the τ_c values increasing as the linker length

2093

dx.doi.org/10.1021/jp211114h | J. Phys. Chem. B 2012, 116, 2090−2095
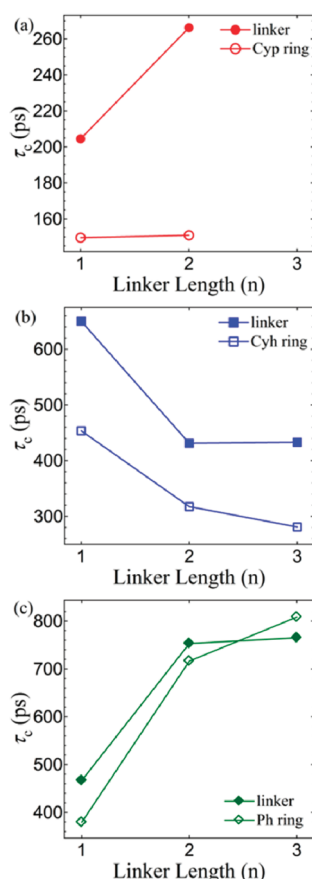
Figure 4. Linker-length dependencies of τ_c values of the linker carbons and average τ_c values of the carbons constituting each substituent for (a) **Cyp[n]NTf$_2$**, (b) **Cyh[n]NTf$_2$**, and (c) **Ph[n]NTf$_2$** at 303 K.

increased. These results indicate that the segmental motion and the entire molecular reorientational motion for **Cyp[n]NTf$_2$** and **Ph[n]NTf$_2$** become slower as the linker length increased. This is consistent with the observed linker-length dependence of the shear viscosities for the series. Thus, it can be concluded that elongation of the linker length in the **Cyp[n]NTf$_2$** and **Ph[n]NTf$_2$** ILs leads to a low mobility for all of the cations as a result of an enhancement of the van der Waals interactions between the linkers. On the other hand, in the case of **Cyh[n]NTf$_2$**, the τ_c's of both linkers and cyclohexyl groups become shorter as the linker lengths increase from $n = 1$ to 2 (Figure 4b), consistent with the variation of the shear viscosities for these ILs. This characteristic linker-length dependence might be attributed to the variation in the mobility of the cyclohexyl group as the linker length increases. The carbons constituting the cyclohexyl group are labeled as C1, C2, C3, and C4, in which C1 is the carbon nearest to the linker and C4 is the farthest one. The τ_c value of C1 at 303 K changes to 532, 316, and 294 ps with the elongation of the linker length from $n = 1$ to 3, respectively. Similar to that for C1, the τ_c values of C2, C3, and C4 also change to 412, 291, 227 ps; 400, 272, 239 ps; and 565, 461, 461 ps, respectively. When the linker is elongated from $n = 1$ to 2, τ_c of C1 becomes considerably shorter, which suggests a substantial increase in the segmental motion of the C1 moiety. This implies that the mobility of the linker and the C1 carbon of **Cyh[1]NTf$_2$** is restricted by the bulky imidazolium cation. The elongation of the linker length from $n = 1$ to 2 provides sufficient motion space, leading to greater mobility in the cyclohexyl group and lower shear

viscosities of **Cyh[2]NTf$_2$**. In contrast, further elongation does not affect the segmental motion of C1 and C4 carbons and the linkers. This result supports the fact that the shear viscosities of **Cyh[n]NTf$_2$** increase with the elongation of the linker length from $n = 2$ to 3.

Furthermore, the linker-length dependence of the τ_c values of the linkers for each series showed good agreement with the corresponding dependence of the shear viscosities. This suggests that the τ_c values of the linkers effectively reflect the entire molecular reorientation. Accordingly, it is found that the mobility of the linkers themselves is strongly restricted by the two bulky substituents, and the linkers have characteristic physicochemical properties distinct from typical n-alkyl chains.

4. CONCLUSION

A series of alkylimidazolium-based ILs incorporating cyclopentyl, cyclohexyl, and phenyl groups as the nonionic substituents on the one end of the alkyl chain were synthesized and characterized with respect to physicochemical properties and reorientational dynamics. By comparison of the imidazolium ILs with various nonionic substituents, it is found that the physicochemical properties of the ILs partially reflect the properties of the nonionic substituents themselves. Contrary to what was observed for the liquid densities, a distinct trend in linker-length dependence was observed for the shear viscosities of each series of imidazolium ILs. The linker-length dependence of τ_c indicates that the elongation of the linker influences the effects of the nonionic substituents on the reorientational dynamics of the system. This result is consistent with macroscopic observations in the shear viscosities. Variations in the τ_c values of the linkers as the linker length increases also imply the characteristic features of the linkers in terms of the mobility.

ASSOCIATED CONTENT

S Supporting Information

Full description of the material. This material is available free of charge via the Internet at http://pubs.acs.org.

AUTHOR INFORMATION

Corresponding Author

*Tel: +81-(0)43-290-3939. Fax: +81-(0)43-290-3939. E-mail: k.nishikawa@faculty.chiba-u.jp.

Notes

The authors declare no competing financial interest.

ACKNOWLEDGMENTS

REFERENCES

(1) Welton, T. *Chem. Rev.* **1999**, *99*, 2071−2083.

(2) Chiappe, C.; Pieraccini, D. *J. Phys. Org. Chem.* **2005**, *18*, 275−297.

(3) Ohno, H. Ed., *Electrochemical Aspects of Ionic Liquids*; Wiley-Interscience: Hoboken, NJ, 2005.

(4) MacFarlane, D. R.; Forsyth, M.; Howlett, P. C.; Prngle, J. M.; Sun, J.; Annat, G.; Neil, W.; Izgorodina, E. I. *Acc. Chem. Res.* **2007**, *40*, 1165−1173.

(5) Smiglak, M.; Metlen, A.; Rogers, R. D. *Acc. Chem. Res.* **2007**, *40*, 1182−1192.

(6) Sun, N.; Rahman, M.; Qin, Y.; Maxim, M. L.; Rodríguez, H.; Rogers, R. D. *Green Chem.* **2009**, *11*, 646−655.

(7) Ye, C.; Liu, W.; Chen, Y.; Yu, L. *Chem. Commun.* **2001**, 2244−2245.

(8) Bônhote, P.; Dias, A. P.; Papageurgiou, N.; Kalyanansundaram, K.; Grätzel, M. *Inorg. Chem.* **1996**, *35*, 1168−1178.

(9) Huddleston, J. G.; Visser, A. E.; Reichert, W. M.; Willauer, H. D.; Broker, G. A.; Rogers, R. D. *Green Chem.* **2001**, *3*, 156−164.

(10) Holbrey, J. D.; Seddon, K. R. *J. Chem. Soc., Dalton Trans.* **1999**, 2133−2139.

(11) Murray, S. M.; O'Brien, R. A.; Mattson, K. M.; Ceccarelli, C.; Sykora, R. E.; West, K. N.; Davis, J. H. Jr. *Angew. Chem., Int. Ed.* **2010**, *49*, 2755−2758.

(12) Xu, W.; Cooper, E. I.; Angell, C. A. *J. Phys. Chem. B* **2003**, *107*, 6170−6178.

(13) Tokuda, H.; Hayamizu, K.; Ishii, K.; Susan, M. A. B. H.; Watanabe, M. *J. Phys. Chem. B* **2004**, *108*, 16593−16600.

(14) Ferrarini, A.; Luckhurst, G. R.; Nordio, P. L.; Roskilly, S. J. *J. Chem. Phys.* **1994**, *100*, 1460−1469.

(15) Emsley, J. W.; Luckhurst, G. R.; Shilstone, G. N.; Sage, I. *Mol. Cryst. Liq. Cryst. Lett.* **1984**, *102*, 223−233.

(16) Barnes, P. J.; Douglass, A. G.; Heeks, S. K.; Luckhurst, G. R. *Liq. Cryst.* **1993**, *13*, 603−613.

(17) Emerson, A. P. J; Luckhurst, G. R. *Liq. Cryst.* **1991**, *10*, 861−868.

(18) Ionescu, D.; Luckhurst, G. R.; Silva, D. S. D. *Liq. Cryst.* **1997**, *23*, 833−843.

(19) Goodby, J. W.; Saez, I. M.; Cowling, S. J.; Gasowska, J. S.; MacDonald, R. A.; Sia, S.; Watson, P.; Toyne, K. J.; Hird, M.; Lewis, R. A.; et al. *Liq. Cryst.* **2009**, *36*, 567−605.

(20) Chung, S.; Parker, J. B.; Bianchet, M.; Amzel, L. M.; Stivers, J. T. *Nat. Chem. Biol.* **2009**, *5*, 407−413.

(21) Bencherif, S. A.; Sheehan, J. A.; Hollinger, J. O.; Walker, L. M.; Matyjaszewski, K.; Washburn, N. R. *J. Biomed. Mater. Res., Part A* **2008**, 142−153.

(22) Anderson, J. L.; Ding, R.; Ellern, A.; Armstrong, D. W. *J. Am. Chem. Soc.* **2005**, *127*, 593−604.

(23) Holbrey, J. D.; Visser, A. E.; Spear, S. K.; Reichert, W. M.; Swatloski, R. P.; Broker, G. A.; Rogers, R. D. *Green Chem.* **2003**, *5*, 129−135.

(24) Shirota, H.; Mandai, T.; Fukazawa, H.; Kato, T. *J. Chem. Eng. Data* **2011**, *56*, 2453−2459.

(25) Yoshizawa, M.; Hirao, M.; Akita, K. I.; Ohno, H. *J. Mater. Chem.* **2001**, *11*, 1057−1062.

(26) Imanari, M.; Nakakoshi, M.; Seki, H.; Nishikawa, K. *Chem. Phys. Lett.* **2008**, *459*, 89−93.

(27) Imanari, M.; Uchida, K.; Miyano, K.; Seki, H.; Nishikawa, K. *Phys. Chem. Chem. Phys.* **2010**, *12*, 2959−2967.

(28) Antony, J. H.; Mertens, D.; Dölle, A.; Wasserscheid, P.; Carper, W. R. *ChemPhysChem* **2003**, *4*, 588−594.

(29) Carper, W. R.; Wahlbeck, P. G.; Dölle, A. *J. Phys. Chem. A* **2004**, *108*, 6096−6099.

(30) Antony, J. H.; Mertens, D.; Breitenstein, T.; Dölle, A.; Wasserscheid, P.; Carper, W. R. *Pure Appl. Chem.* **2004**, *76*, 255−261.

(31) Mandai, T.; Imanari, M.; Nishikawa, K. *Chem. Phys. Lett.* **2011**, *507*, 100−104.

(32) Stracke, M. P.; Ebeling, G.; Cataluna, R.; Dupont, J. *Energy Fuels* **2007**, *21*, 1695−1698.

(33) A short history of SHELX: Sheldrick, G. M. *Acta Crystallogr.* **2008**, *A64*, 112−122.

(34) Lide, D. R., Ed. *CRC Handbook of Chemistry and Physics*, 90th ed.; CRC Press: Boca Raton, FL, 2009.

(35) Holbrey, J. D.; Reichert, W. M.; Rogers, R. D. *Dalton Trans.* **2004**, 2267−2271.

(36) Bondi, A. *J. Phys. Chem.* **1964**, *68*, 441−451.

(37) Edward, J. T. *J. Chem. Educ.* **1970**, *47*, 261−270.

(38) Mandai, T.; Masu, H.; Imanari, M.; Nishikawa, K. *J. Phys. Chem. B* **2012**, DOI: 10.1021/jp210273q.

(39) Bini, R.; Malvaldi, M.; Pitner, W. R.; Chiappe, C. *J. Phys. Org. Chem.* **2008**, *21*, 622−629.

(40) Jensen, F. R.; Noyce, D. S.; Sederholm, C. H.; Berlin, A. J. *J. Am. Chem. Soc.* **1962**, *84*, 386−389.

(41) Perrin, C. L.; Fabian, M. A.; Armstrong, K. B. *J. Org. Chem.* **1994**, *59*, 5246−5253.

(42) Imanari, M.; Tsuchiya, H.; Seki, H.; Nishikawa, K.; Tashiro, M. *Magn. Reson. Chem.* **2009**, *47*, 67−70.

(43) Solomon, I. *Phys. Rev.* **1955**, *99*, 559−565.

(44) Hayamizu, K.; Tsuzuki, S.; Seki, S. *J. Phys. Chem. B* **2008**, *112*, 12027−12036.